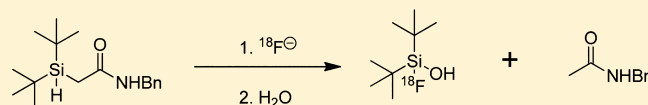


Studies toward the Development of New Silicon-Containing Building Blocks for the Direct ^{18}F -Labeling of PeptidesLukas O. Dialer,[†] Svetlana V. Selivanova,[†] Carmen J. Müller,[†] Adrienne Müller,[†] Timo Stellfeld,[‡] Keith Graham,[‡] Ludger M. Dinkelborg,^{‡,||} Stefanie D. Krämer,[†] Roger Schibli,[†] Markus Reiher,[§] and Simon M. Ametamey^{*,†}[†]Center for Radiopharmaceutical Sciences of ETH, PSI and USZ, Department of Chemistry and Applied Biosciences, Swiss Federal Institute of Technology (ETH) Zurich, Wolfgang-Pauli Strasse 10, CH-8093, Zurich, Switzerland[‡]Global Drug Discovery, Bayer Healthcare, Muellerstrasse 178, 13353 Berlin, Germany[§]Laboratory of Physical Chemistry, Department of Chemistry and Applied Biosciences, Swiss Federal Institute of Technology (ETH) Zurich, Wolfgang-Pauli Strasse 10, CH-8093, Zurich, Switzerland

Supporting Information

ABSTRACT: Silicon-containing prosthetic groups have been conjugated to peptides to allow for a single-step labeling with ^{18}F radioisotope. The fairly lipophilic di-*tert*-butylphenylsilane building block contributes unfavorably to the pharmacokinetic profile of bombesin conjugates. In this article, theoretical and experimental studies toward the development of more hydrophilic silicon-based building blocks are presented. Density functional theory calculations were used to predict the hydrolytic stability of di-*tert*-butylfluorosilanes **2–23** with the aim to improve the in vivo properties of ^{18}F -labeled silicon-containing biomolecules. As a further step toward improving the pharmacokinetic profile, hydrophilic linkers were introduced between the lipophilic di-*tert*-butylphenylsilane building block and the bombesin congeners. Increased tumor uptake was shown with two of these peptides in xenograft-bearing mice using positron emission tomography and biodistribution studies. The introduction of a hydrophilic linker is thus a viable approach to improve the tumor uptake of ^{18}F -labeled silicon–bombesin conjugates.



INTRODUCTION

Radiolabeled biomolecules such as proteins and peptides have been applied for positron emission tomography (PET) imaging due to their fast and specific targeting properties.^{1–3} Often, metal radioisotopes are used to radiolabel biomolecules using chelators which allow for highly efficient labeling under mild conditions.⁴ However, fluorine-18 (^{18}F) generally possesses better nuclear characteristics for PET due to the low positron (β^+) energy (0.64 MeV), including an appropriate physical half-life (109.7 min).^{5,6} Procedures for the direct labeling with ^{18}F normally require harsh (strong bases, high temperatures) reaction conditions which are not compatible with sensitive biomolecules.⁵ Usually, site-specific labeling of peptides or proteins with ^{18}F is achieved using suitable ^{18}F -labeled intermediates or prosthetic groups.^{7–10} This approach includes multistep reaction procedures and is, therefore, time-consuming. A more efficient, one-step procedure for radio-fluorination under mild conditions would be beneficial to accommodate for the short half-life of ^{18}F and the lability of peptides. Great advancements have been made in recent years in ^{18}F labeling using organoboron, aluminum chelate, and 4-trimethylammonium-3-cyano-benzoyl moiety bearing bioconjugates.^{11–13}

Application of prosthetic groups containing silicon for site-specific ^{18}F labeling of peptides and other biomolecules was investigated in our laboratory and by others.^{14–18} Because of a

high silicon–fluorine (Si–F) bond energy (565 vs 485 kJ mol^{−1} for carbon–fluorine (C–F) bond), silicon has a high affinity for fluorine and is easily fluorinated, allowing for a direct one-step labeling under mild conditions.^{16,19} However, the Si–F bond is prone to dissociation in the presence of water. To shield the Si–F bond from hydrolysis, bulky lipophilic di-*tert*-butyl groups were employed for the design of the currently used di-*tert*-butylphenylsilyl building block. Di-*tert*-butylphenylsilyl, in turn, confers its high lipophilicity to the final peptide conjugate. In vivo studies in mice using bombesin derivatives labeled with ^{18}F via di-*tert*-butylphenylsilyl building block confirmed that high lipophilicity of the final conjugate negatively affected its systemic distribution and revealed only low and unspecific uptake in gastrin-releasing peptide receptor (GRPr) positive xenografts.²⁰ Bombesin and its derivatives exhibit high affinity and selectivity for the GRPr, which is overexpressed in various human tumors including prostate, breast, pancreatic, and small cell lung cancers.^{21–23} A reduction of the overall lipophilicity may lead to an improved pharmacokinetic profile of the radiolabeled peptide by shifting hepatobiliary to renal clearance.

In the present study, we report the synthesis and evaluation of silicon containing compounds with enhanced hydrophilic

Received: April 5, 2013

properties. Stability of the Si–F bond toward hydrolysis was predicted using density functional theory (DFT) calculations and tested experimentally. Modification of the linker between the di-*tert*-butylphenylsilyl building block and bombesin analogues

was also investigated. Two bombesin analogues were radio-fluorinated using a one-step labeling protocol and tested for their binding affinity in vitro and their performance in vivo in mice.

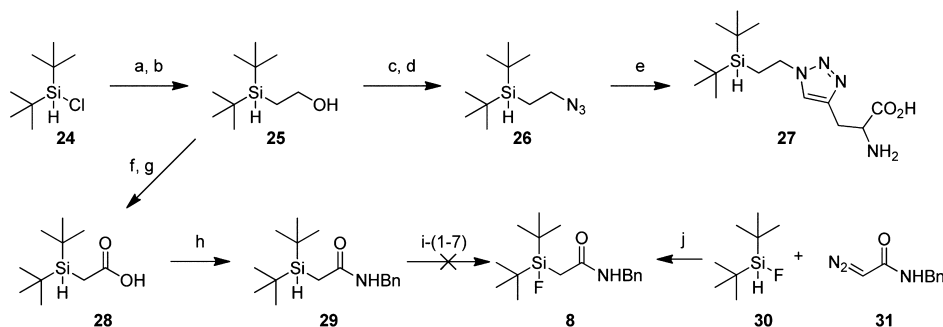
Table 1. Silicon-Based Building Blocks 1–23 with Their cLogP Values, Experimentally Evaluated Hydrolytic $t_{1/2}$, and Calculated $\Delta_{(\text{Si-F})}$ Values

Compound	Structure	cLogP	Hydrolytic $t_{1/2}$	$\Delta_{(\text{Si-F})}$ [Å]
1 ¹⁹		5.56	> 300 h	0.18
2		2.51	8 h	0.21
3		2.84	n/d	0.21
4		3.91	n/d	0.19
5		4.22	n/d	0.24
6		1.95	n/d	0.18, 0.27 ^a
7		2.25	n/d	0.25, 0.19 ^a
8		4.10	n/d	0.25, 0.23 ^a
9		4.39	n/d	0.22
10		2.30	n/d	0.20
11		2.61	n/d	0.20
12		4.19	n/d	0.19
13		4.35	n/d	0.20
14		3.12	n/d	0.17
15		3.18	n/d	0.21
16		-0.08	n/d	0.24
17		0.25	n/d	0.21

Table 1. continued

Compound	Structure	cLogP	Hydrolytic $t_{1/2}$	$\Delta_{(\text{Si-F})}$ [Å]
18		-0.94	16 h	0.21
19		-0.73	n/d	0.23
20		1.77	n/d	0.18
21		2.37	n/d	0.20
22		2.52	n/d	0.20
23		2.86	n/d	0.20

^a $\Delta_{(\text{Si-F})}$ values of DFT structure optimizations of isomers, for which the starting structure guaranteed convergence to a stable conformer free of intramolecular hydrogen bonds.

Scheme 1. Synthesis of Silylethanol 25, Triazole Amino Acid 27, Silylacetamide 29, and Fluorosilylacetamide 8^a

^aReagents and conditions: (a) $\text{N}_2\text{CHCO}_2\text{Et}$, $\text{Rh}_2(\text{OAc})_4$, DCM, 35 °C; (b) LAH, THF, 0 °C to reflux, 64% (two steps); (c) PPh_3 , CBr_4 , DCM, 0 °C to rt; (d) NaN_3 , DMF, 57% (two steps); (e) propargyl glycine, $\text{Cu}(\text{II})$ acetate, (+)-sodium L-ascorbate, $^t\text{BuOH}/\text{water}$, 22%; (f) PCC, DCM; (g) NaO_2Cl , sulfamic acid, acetone/water, 0 °C, 26% (two steps); (h) BnNH_2 , DIPEA, T3P, THF, 0 °C to rt, 35%; (i-1) KF, K222, THF or toluene, rt, (i-2) KF, K222, AcOH, THF, rt or reflux, (i-3) KF, K222, K_2CO_3 , (i-4) TBAF, THF, with or without AcOH, (i-5) TBABF, KHF_2 , THF, (i-6) CuF_2 , CCl_4 , (i-7) CuCl_2 , CuI, KF, Et_2O , (j) $\text{Rh}_2(\text{OAc})_4$, DCM, 5%.

RESULTS

DFT Calculations. The difference in Si–F bond lengths ($\Delta_{(\text{Si-F})}$) of the silane and its solvated hydrolysis intermediate was obtained using DFT calculations (see the Experimental Section for the computational methodology). The $\Delta_{(\text{Si-F})}$ values for model silane compounds 2–23 are depicted in Table 1. Fluorosilanes 6, 14, and 20 show $\Delta_{(\text{Si-F})}$ values below 0.19 Å and are predicted to be hydrolytically stable according to our previous discussion in Höhne et al.¹⁹ Fluorosilanes 2–5, 7–13, 15–19, and 21–23 all exhibit a $\Delta_{(\text{Si-F})}$ value ≥ 0.19 Å and were therefore considered to be hydrolytically unstable.

When re-evaluating model compounds 6, 7, and 8, we observed that in the microsolvated intermediate structure the –NH– group in one of the silicon substituents formed a hydrogen bond to the OH^- moiety and/or to the water molecule, respectively. In the former case, the Si–F bond elongation was reduced resulting in a smaller $\Delta_{(\text{Si-F})}$ value, while the opposite occurred in the latter case. To investigate how strong these

intramolecular hydrogen bonds are, we performed additional calculations using the shared-electron-numbers (SENs) method²⁴ and found hydrogen bond energies of 21.4, 16.0, and 13.3 kJ/mol for silanes 6, 7, and 8, respectively. DFT calculations for compounds 6, 7, and 8 were newly performed in such a way that these intramolecular hydrogen bonds were broken to have a different stable conformer. The new $\Delta_{(\text{Si-F})}$ values were 0.27, 0.19, and 0.23 Å for silanes 6, 7 and 8, respectively, and are assigned with the footnote (a) in Table 1.

Chemistry. The syntheses of silanes 8, 25, 27, and 29 were accomplished as shown in Scheme 1. Di-*tert*-butylchlorosilane (24) was reacted with ethyl diazoacetate in the presence of a rhodium(II) catalyst via a rhodium carbene complex. The obtained silylethylester was further reduced with LAH to yield silylethanol 25 in 64% yield over two steps. Primary alcohol 25 was brominated using triphenylphosphine and carbon tetrabromide. The obtained bromide was converted to azide 26 in 57% yield. Coupling with L-propargylic glycine via copper-catalyzed

azide–alkyne cycloaddition (CuAAC) afforded triazole **27** in 22% yield. Silylethanol **25** was treated with PCC to form the intermediate aldehyde, which was subsequently oxidized with sodium chlorite and sulfamic acid to carboxylic acid **28** in 26% yield. Coupling of **28** to benzyl amine with 2,4,6-triisopropyl-1,3,5,2,4,6-trioxatriphosphorinane 2,4,6-trioxide (T3P) afforded silylamide **29** in 35% yield. Fluorosilyl amide **8** was synthesized by reacting fluorosilane **30** with diazoacetamide **31** using a rhodium(II) catalyst, whereas direct fluorination of silane **29** using various reagents and conditions was not successful (Scheme 1, i-(1–7)). NMR studies showed complete decomposition of **8** after seven days in CDCl₃ (probably promoted by the moisture in the NMR tube and/or the presence of DCl/HCl traces in CDCl₃). Decomposition products were identified by NMR analysis to be di-*tert*-butylfluorosilanol (**32**) and *N*-benzylacetamide (**33**) as illustrated in Figure 1.

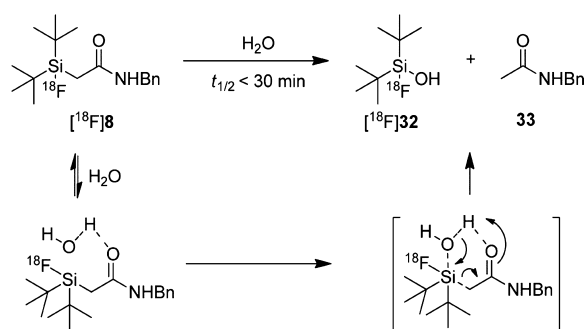


Figure 1. Proposed mechanism for the hydrolysis of [¹⁸F]**8**.

The synthetic pathway leading to silane **36** and fluorosilane **37** is shown in Scheme 2. Primary amine **34** was protected with the BOC-group using di-*tert*-butyl dicarbonate to afford compound **35** in quantitative yield. Bromoaryl **35** was treated with *n*-butyllithium (*n*-BuLi), and the resulting lithiate was trapped by di-*tert*-butylchlorosilane to give the intermediate silylaryl compound. Deprotection of the primary amine under acidic conditions and further reaction with di-*O*-acetyl-tartaric acid anhydride yielded silane **36** in 21% yield. Direct fluorination of silane **36** with potassium fluoride (KF) in the presence of Kryptofix 222 (K222) and acetic acid (AcOH) gave fluorosilane **37** in 36% yield.

Peptide Synthesis and in Vitro Receptor Binding Assay. Peptide synthesis was carried out using Rink amide resin following standard Fmoc strategy.²⁵ The conjugation of the

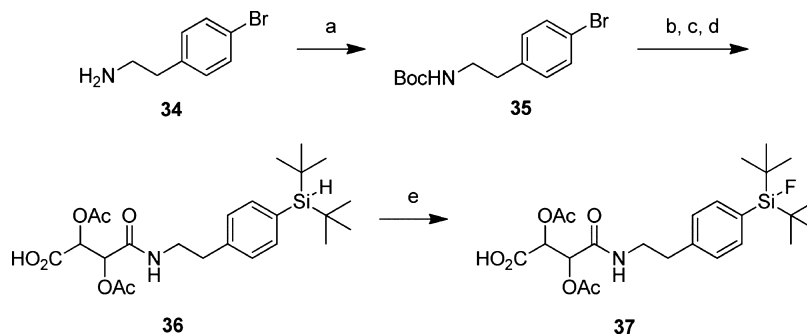
resin-bound peptide with 2-(4-(di-*tert*-butylsilyl)phenyl)acetic acid required a coupling reagent system (HBTU (*O*-(benzotriazol-1-yl)-*N,N,N,N*-tetramethyluronium hexafluorophosphate) and HOBT (1-hydroxybenzotriazole)/DIPEA (*N,N*-diisopropylethylamine)). Nonradioactive reference compound **39** (Figure 2) was obtained by direct fluorination of precursor **38** with KF in the presence of K222 and glacial acetic acid. Higher yields for peptides **41** and **43** were obtained when DMTMM-BF₄ (4-(4,6-dimethoxy-1,3,5-triazin-2-yl)-4-methylmorpholinium tetrafluoroborate) and NMM (*N*-methylmorpholine) were used as coupling reagents. Fluorosilane **43** contained impurities of silanol **44** (**44**/**43** = 3:1). The IC₅₀ values determined for peptides **39** and **41** were 8.3 ± 1.4 and 23 ± 13 nM, respectively.

Radiolabeling, Hydrolytic Stability of the Si–¹⁸F Bond, and log D_{7.4} Measurement. The direct ¹⁸F-fluorination protocol developed previously in our laboratory²⁰ was applied for the radiolabeling of hydrosilanes **25**, **27**, and **29** as depicted in Scheme 3. ¹⁸F-Incorporation of >95% was achieved for all these hydrosilanes. The measured hydrolytic half-lives of [¹⁸F]**2** and [¹⁸F]**18** in the presence of water were 8 and 16 h, respectively. For both compounds, hydrolysis was much faster in PBS or in 0.9% NaCl than in water. ¹⁸F-Labeling of **29** gave *N*-benzylacetamide (**33**) and di-*tert*-butyl[¹⁸F]fluorosilanol ([¹⁸F]**32**) instead of [¹⁸F]**8**.

A similar labeling approach was used for the radiosynthesis of peptides [¹⁸F]**39** and [¹⁸F]**43**. For both peptides, the best ¹⁸F-incorporation yield was obtained when 10 μL of acetic acid was used as an additive. Then 32 GBq ¹⁸F[−] provided 350 MBq of [¹⁸F]**39** with a specific radioactivity of 35 GBq/μmol at the end of synthesis (EOS). Then 190 MBq of [¹⁸F]**43** with a specific radioactivity of 70 GBq/μmol (EOS) was produced starting from 30 GBq ¹⁸F[−]. Both peptides were stable in PBS over 2 h. The logarithmic distribution coefficient (log D_{7.4}) value as a measure of lipophilicity was determined by the shake flask method and amounted to 0.3 ± 0.1 (*n* = 3) for [¹⁸F]**39**. The lipophilicity of [¹⁸F]**43** was not determined.

Small Animal PET. PET images of human prostate adenocarcinoma (PC-3) xenograft-bearing mice after injection of [¹⁸F]**39** and [¹⁸F]**43**, respectively, are shown in Figure 3. The highest radioactivity concentrations for both radiolabeled peptides were observed in the abdominal region in all tested mice. The tumors were clearly visualized with both [¹⁸F]**39** and [¹⁸F]**43** (Figures 3A,C,D), consistent with the ex vivo biodistribution data (see next Ex Vivo Biodistribution). Co-injection of [¹⁸F]**39** with 50 μg of bombesin resulted in a reduction of radioactivity uptake in the tumor (Figure 3B).

Scheme 2. Synthesis of Silane **36** and Fluorosilane **37**^a



^aReagents and conditions: (a) Boc₂O, NEt₃, CH₃OH, 0 °C to rt, quant; (b) *n*-BuLi, THF, ^tBuSiHCl (**16**), −78 °C to rt; (c) 1.25 M HCl/CH₃OH, rt; (d) di-*O*-acetyl-tartaric acid anhydride, NEt₃, CoCl₂(cat), CH₃CN, 21% (three steps); (e) KF, K222, AcOH, THF, reflux, 36%.

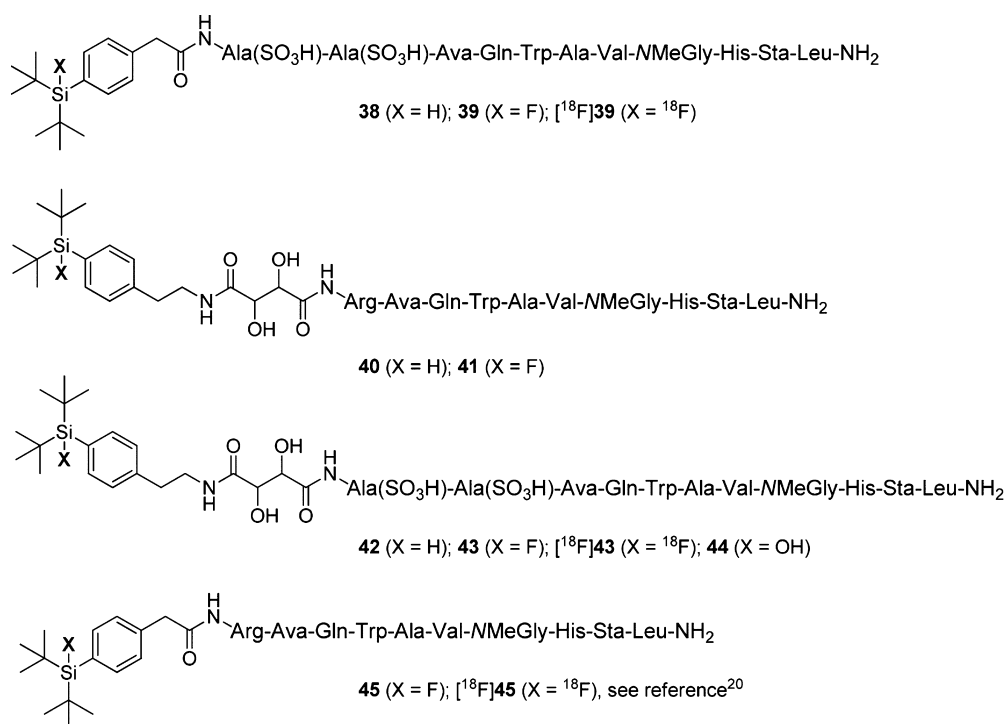
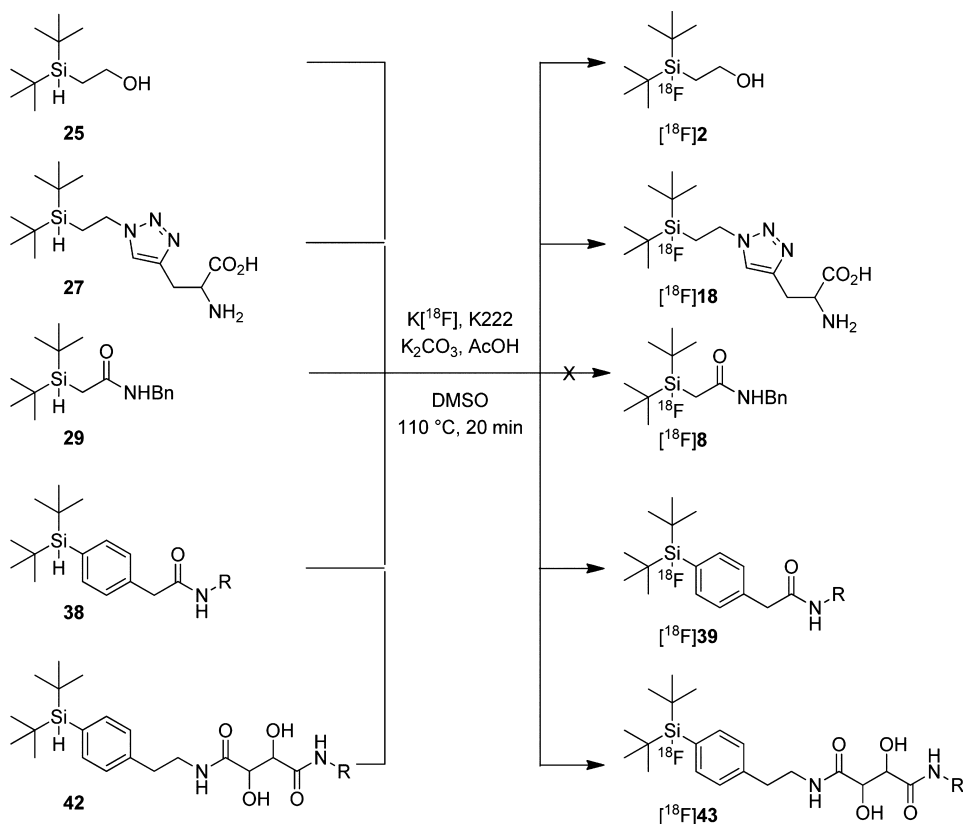


Figure 2. Structures of silicon containing bombesin analogues.

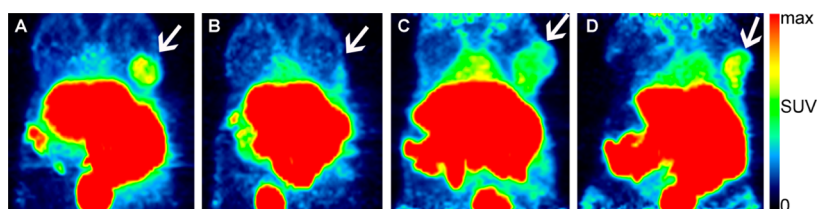
Scheme 3. ^{18}F -Radiolabeling of Model Compounds 25, 27, and 29 and of Peptides 38 and 42^a



^aR = Ala(SO₃H)-Ala(SO₃H)-Ava-Gln-Trp-Ala-Val-NMeGly-His-Sta-Leu-NH₂.

Ex Vivo Biodistribution. Tables 2 and 3 summarize the ex vivo biodistribution data of [^{18}F] 39 and [^{18}F] 43 in PC-3 xenograft-bearing mice, which were sacrificed after PET imaging. The tumor uptake of [^{18}F] 39 was $1.8 \pm 0.7\%$ ID/g ($n = 3$) at 117 min

after injection and was reduced by coinjection of nonradioactive bombesin ($50 \mu\text{g}$ per mouse) to $1.24 \pm 0.09\%$ ID/g ($n = 3$). Tumor to blood ratio was 2.0 at baseline and was reduced to 1.1 under blocking conditions. The gallbladder uptake of [^{18}F] 39



^aMaximum intensity projections. ^bArrows point at PC-3 tumor xenografts. ^cImage data were normalized to SUV (A,B, $SUV_{max} = 2$; C,D, $SUV_{max} = 4$). **Figure 3.** PET images (MIP)^a with [¹⁸F]39 (60–105 min pi) under baseline (A) and blocking (B) conditions and with [¹⁸F]43 (C, 62–92 min pi; D, 140–170 min pi) under baseline conditions^{b,c}

Table 2. Ex Vivo Biodistribution of [¹⁸F]39 in PC-3 Tumor-Bearing Mice in Comparison to Previously Reported Data of [¹⁸F]45

tissue and ratio	[¹⁸ F]39 ^a		[¹⁸ F]45 ^b
	baseline [%ID/g]	blockade [%ID/g]	baseline [%ID/g]
tumor	1.8 ± 0.7	1.24 ± 0.09	0.40 ± 0.05
blood	0.91 ± 0.14	1.17 ± 0.08	0.42 ± 0.04
pancreas	10 ± 5	3.4 ± 0.5	4.08 ± 0.67
prostate	0.37 ± 0.16	0.7 ± 0.6	n/d
liver	4.4 ± 1.2	5.6 ± 0.4	4.40 ± 1.04
kidney	1.7 ± 0.8	2.1 ± 0.7	1.73 ± 0.24
intestine	21 ± 12	16 ± 9	16 ± 4
lung	0.65 ± 0.12	1.4 ± 0.4	n/d
gallbladder	194 ± 12	236 ± 78	146 ± 126
spleen	0.57 ± 0.25	0.57 ± 0.24	0.46 ± 0.06
tumor/blood	2.0	1.1	0.95

^aBiodistribution at 117 min pi under baseline (8.3–15.3 MBq, $n = 3$) and blocking conditions (4.8–10.5 MBq, $n = 3$). ^bBiodistribution at 120 min pi under baseline conditions.²⁰

was $194 \pm 12\%$ ID/g, indicating hepatobiliary clearance of [¹⁸F]39. [¹⁸F]43 showed tumor uptake of 3.5%ID/g (104 min post-injection (pi)) and 2.4%ID/g (182 min pi), respectively. The tumor to blood ratio (0.9) was higher at 182 min pi than at 104 min pi, and tumor to muscle ratios at 104 min and at 182 min

after injection were 5 and 8, respectively. Because of the lower tumor to blood ratio and the higher radioactivity values in blood, liver, and kidneys, we did not further investigate the specificity of [¹⁸F]43. As expected for both peptides, a high accumulation of radioactivity was measured in the pancreas, adrenal glands, and intestines due to the high physiological expression of GRPr in these organs.

DISCUSSION

Previous studies by both our group and the Schirmacher group have documented the importance of the *tert*-butyl substituents for designing hydrolytically stable silicon building blocks.^{14,19} Therefore, in our approach to design new building blocks with reduced lipophilicity, we have decided to retain two *tert*-butyl substituents and to replace the aromatic part of the new building blocks with less lipophilic moieties. Previous DFT calculations by Höhne et al. showed that compounds with $\Delta_{(Si-F)} \geq 0.19$ Å tend to be unstable in aqueous solutions, while compounds with $\Delta_{(Si-F)} < 0.19$ Å are considered to be hydrolytically stable.¹⁹

In the present study, DFT calculations showed that model compounds 2–23 exhibit $\Delta_{(Si-F)}$ values ≥ 0.19 Å, except compounds 6, 14, and 20, which all have $\Delta_{(Si-F)}$ values below 0.19 Å (Table 1). No correlation exists between the lipophilicity of the building blocks and their $\Delta_{(Si-F)}$ values. To verify the theoretical calculations, precursors 25, 27, and 29 of model compounds 2, 8, and 18, respectively, were labeled with ¹⁸F[−] (Scheme 3) and

Table 3. Ex Vivo Biodistribution of [¹⁸F]43 in PC-3 Tumor-Bearing Mice

tissue and ratios	[¹⁸ F]43	
	baseline (104 min pi) [%ID/g]	baseline (182 min pi) [%ID/g]
tumor	3.47	2.44
blood	5.37	2.58
pancreas	46	21
prostate	0.44	0.29
liver	25	13
kidney	6	4.1
intestine	12.6	9.5
lung	4.2	1.94
gallbladder	36	128
urine	25	20
spleen	2.15	1.32
heart	1.37	0.85
fat	1.24	0.51
muscle	0.69	0.29
adrenal gland	5.01	2.07
bone	1.09	0.92
stomach	0.42	0.8
tumor/blood	0.65	0.95
tumor/muscle	5.03	8.41

subjected to hydrolytic stability studies. The predicted hydrolytic instability of the Si–¹⁸F bond of [¹⁸F]**2** and [¹⁸F]**18** in aqueous solutions could be confirmed experimentally. On the basis of these results, we did not further synthesize reference compounds **2** and **18** and we conclude that relatively fast hydrolysis of the Si–F bond of these compounds takes place due to a decreased steric hindrance around the silicon atom. This may also explain the greater than 0.19 Å $\Delta_{(\text{Si-F})}$ values for **3–5**, **7–13**, **15**, **17–19**, and **21–23**. Replacement of the phenyl ring by a similarly bulky triazole ring increased the $\Delta_{(\text{Si-F})}$ value to 0.24 Å as calculated for **16**. This might be due to the basic triazole nitrogen atoms, which enhance the nucleophilic character of surrounding water molecules and thus facilitate hydrolysis of the Si–F bond. Because of the hydrolytic instability of triazole **16**, its “click” precursor acetylene **14** with a $\Delta_{(\text{Si-F})}$ value of 0.17 Å was not further investigated although **14** is predicted to be hydrolytically stable. Methoxymethoxysilanes **20** and **21** differ only in their terminal group and thus it is reasonable to assume that the remote functionalities might have influenced their $\Delta_{(\text{Si-F})}$ values. Compound **20** with an advantageous $\Delta_{(\text{Si-F})}$ value of 0.18 Å was not further evaluated because it is synthetically not easily accessible.

The hydrolytic stability of acetamide **6** was verified using model compound **8**. Unexpectedly, ¹⁸F-labeling of precursor compound **29** which was anticipated to afford [¹⁸F]**8** did not lead to the desired radiolabeled compound but instead to di-*tert*-butyl[¹⁸F]fluorosilanol ([¹⁸F]**32**) and *N*-benzylacetamide (**33**). Mechanistically, we assume fluorosilane [¹⁸F]**8** undergoes hydrolysis corresponding to a mechanism described for the solvolysis of β -ketosilanes.²⁶ According to this mechanism, the silicon–methylene (Si–CH₂) bond of [¹⁸F]**8** is cleaved instead of the Si–F bond (Figure 1). In the future, we plan to focus DFT calculations not only on the stability of Si–F bond but also to evaluate the stability of all silicon–carbon bonds.

In the DFT calculation of microsolvated intermediate model structures, from which we extracted one Si–F bond length needed for the $\Delta_{(\text{Si-F})}$ measure, we assumed that a hydroxide anion (OH[−]) binds to the silicon atom, while a water molecule builds up a hydrogen bond to the fluorine atom of the compounds.¹⁹ Hence, the measured elongation of the Si–F bond depends on both the binding of OH[−] and the hydrogen bond of the water molecule. However, we use a small microsolvated model system for the intermediate in which strong intramolecular hydrogen bonds can be expected to lead to artifacts in the interpretation. In contrast, intramolecular hydrogen bonds are not likely to occur in aqueous solution as other water molecules can saturate these contacts, thus making their formation very difficult if not impossible. Therefore, we propose that $\Delta_{(\text{Si-F})}$ values of conformers *without* intramolecular hydrogen bonds are more suitable to predict the hydrolytic stability of Si–F bonds. Accordingly, we changed the intermediate conformations of model compounds **6**, **7**, and **8** in order to make sure that no intramolecular hydrogen bonds occurred in our microsolvated structures. The new $\Delta_{(\text{Si-F})}$ values differed a lot from the $\Delta_{(\text{Si-F})}$ values of the conformers *with* intramolecular hydrogen bonding showing the influence of neglecting intramolecular hydrogen bonds in the calculations. However, the $\Delta_{(\text{Si-F})}$ values of **6** and **8** are not similar and we lack a reasonable explanation for this discrepancy.

One possibility to compensate for the high lipophilicity of the di-*tert*-butylsilylphenyl building block is to introduce hydrophilic linkers between the peptide sequence and the silicon containing building block. This strategy has successfully been applied by

Schirmacher and his co-workers for silicon-based carbohydrate-conjugated octreotate derivatives.²⁷ As a proof of concept, we selected the previously investigated peptide **45**²⁰ and replaced the arginine linker by two *L*-cysteic acids (Ala(SO₃H)) to give **39** as shown in Figure 2. In addition, incorporation of hydrophilic tartaric acid between arginine or *L*-cysteic acid and the silicon building block afforded peptides **41** and **43**. The synthesis of silicon building block **36** is shown in Scheme 2. The binding affinities (IC₅₀) of **39** and **41** determined in competition assays with [¹²⁵I]-Tyr⁴-bombesin were 8.3 ± 1.4 and 23 ± 13 nM, respectively, and found to be comparable to previously reported ¹⁸F-labeled bombesin analogues **45** (IC₅₀ = 22.9 nM) and FB-[Lys³]-bombesin (IC₅₀ = 5.3 nM).^{20,28} The binding affinity of **43** was not determined as several attempts to produce pure **43** failed, mainly due to difficulties in separating **43** from its silanol counterpart **44**. However, we anticipate that the IC₅₀ value of **43** would be in the same range as peptide **39** because **39** and **43** differ only in the linker, which does not participate in the binding to the GRPr. The radiosyntheses of peptides [¹⁸F]**39** and [¹⁸F]**43** were accomplished via a one-step reaction using hydride as a leaving group (Scheme 3). Both [¹⁸F]**39** and [¹⁸F]**43** were produced in sufficient radiochemical yields, specific radioactivity, and good radiochemical purity for animal experiments. The log *D*_{7.4} value for [¹⁸F]**39** was 0.3 ± 0.1, which is 1 unit lower than the log *D*_{7.4} value of [¹⁸F]**45** (log *D*_{7.4} = 1.3 ± 0.1).²⁰

PET studies showed that [¹⁸F]**39** accumulated in the tumor but to a greater extent in the abdominal region and the urinary bladder. Bone uptake was not observed and thus defluorination did not occur. The tumor was not visualized under blocking conditions and the GRPr expressing pancreas was slightly blocked in ex vivo biodistribution. Compared to the ex vivo biodistribution data of [¹⁸F]**45**, the more hydrophilic [¹⁸F]**39** showed a 4.5-fold higher tumor accumulation and a 2-fold higher tumor to blood ratio at 120 min pi but still moderate specificity. Preliminary *ex vivo* biodistribution studies of [¹⁸F]**43** revealed a 1.4–1.9-fold higher accumulation than for [¹⁸F]**39**. However, substantially higher liver uptake was also observed and the tumor to blood ratio was 3.1–2.1-fold lower than with [¹⁸F]**39**. Nevertheless, our hypothesis that increased hydrophilicity of the conjugate will facilitate tumor uptake compared to [¹⁸F]**45** was confirmed.

CONCLUSION

In the present study, several silicon-based building blocks with enhanced hydrophilic properties were investigated. None of the synthesized compounds preserved their stability in aqueous solution. An overall enhanced hydrophilicity of the silicon-containing peptide through modification of the linker leads to an improved pharmacokinetic profile and to an enhanced tumor uptake. Greater improvements may be achieved if a hydrolytically stable silicon-based building block with significantly reduced lipophilicity would become available.

EXPERIMENTAL SECTION

DFT Calculations. The DFT calculations to predict the hydrolytic stability of the Si–F bond in fluorosilanes **2–23** (Table 1) were carried out according to the previously published method.¹⁹ Briefly, a S_N2 mechanism for the hydrolysis of the Si–F bond occurring under inversion via a pentacoordinate intermediate is assumed. The difference of the calculated Si–F bond lengths of the fluorosilane and its corresponding fluorosilanol pentacoordinate intermediate provides the $\Delta_{(\text{Si-F})}$ value. The all-electron Kohn–Sham DFT calculations were performed using the quantum-chemical program package Turbomole.²⁹

The pure functional TPSS in combination with the resolution-of-identity ("RI") density fitting technique, and the def-TZVP basis set for all atoms apart from Si were applied.^{30,31} For Si, we used a def-TZVPP basis set³⁰ with Dunning-type polarization functions as implemented in Turbomole 6.4. To estimate intramolecular hydrogen bond energies, we employed the SENs approach by Reiher et al.²⁴ For this, single-point BP86/RI/TZVP calculations, as described in ref 24 were carried out on top of the TPSS-optimized structures.

Chemistry. All reactions were carried out under an atmosphere of argon in oven-dried glassware with magnetic stirring, unless otherwise indicated. The reagents and solvents were purchased from Sigma-Aldrich Chemie GmbH, Fluka Chemie AG, Archimica GmbH, Chemie Brunschwig AG, Acros Organics, ABCR GmbH & Co., or VWR International AG and were used as supplied unless stated otherwise. Flash chromatography was performed with Fluka silica gel 60 (0.040–0.063 μm grade). Analytical TLC was performed with commercial aluminum sheets coated with 0.25 mm silica gel (E. Merck, Kieselgel 60 F254). Compounds were visualized by UV light at 254 nm and by dipping the plates in an aqueous potassium permanganate solution or in an ethanolic vanillin/sulfuric acid solution followed by heating. ¹H, ¹³C, ¹⁹F, and ²⁹Si NMR data were acquired on a Bruker AV400 (400 MHz) or AV500 (500 MHz) spectrometer. Chemical shifts are reported in delta (δ) units, in parts per million (ppm) downfield from tetramethylsilane (¹H NMR and ²⁹Si NMR), from trichlorofluoromethane (¹⁹F NMR) and relative to the center line of a triplet at 77.0 ppm for chloroform-*d* (¹³C NMR). Splitting patterns are designated as: s, singlet; d, doublet; t, triplet; q, quartet; m, multiplet; br, broad peaks. All coupling constants (*J*) are given in Hz. IR data were recorded on a Perkin-Elmer, Spectrum 100, FT-IR spectrometer. Absorbance frequencies are reported in reciprocal centimeters (cm^{-1}). HRMS were performed by the MS service at the Laboratory of Organic Chemistry, ETH Zurich, and are given in *m/z*.

2-(Di-*tert*-butylsilyl)ethanol (25). To a mixture of di-*tert*-butylchlorosilane (**24**, 5.3 mL, 26 mmol) and rhodium(II) acetate dimer (0.11 g, 0.25 mmol) in dry DCM (14 mL) a solution of ethyl diazoacetate (4.8 mL, 39 mmol) was added slowly over 7 h at 35 °C. The mixture was filtered through Celite (DCM) and concentrated in vacuo. The residue was added dropwise to a mixture of LAH (5.6 g, 147 mmol) in THF (74 mL) at 0 °C. After heating at reflux for 2.5 h, the reaction was quenched with 1 M HCl, diluted with ethylacetate (EtOAc), and filtered. The organic phase was washed with 1 M HCl (1 \times), water (1 \times), and brine (1 \times) and dried over MgSO₄. The residue was purified by flash column chromatography on silica gel (19:1 \rightarrow 4:1, hexane/EtOAc) to yield **25** (3.14 g, 64% over two steps) as colorless liquid. *R*_f 0.43 (7:3, hexane/EtOAc). ¹H NMR (400 MHz, CDCl₃) δ 3.82–3.77 (m, 2H, CH₂OH), 3.28 (t, *J* = 2.7 Hz, 1H, SiH), 1.52 (s, 1H, OH), 1.09–1.01 (m, 2H, SiCH₂), 1.00 (s, 18H, CH₃). ¹³C NMR (100 MHz, CDCl₃) δ 61.6, 28.6, 18.6, 14.8. ²⁹Si NMR (CDCl₃, 99 MHz) δ 8.4.

(2-Azidoethyl)di-*tert*-butylsilane (26). Triphenylphosphine (306 mg, 1.17 mmol) was slowly added to a solution of **25** (200 mg, 1.06 mmol) in DCM (5.3 μL) at 0 °C. After 5 min of stirring, carbon tetrabromide (387 mg, 1.17 mmol) was added slowly. The reaction was stirred for 10 min at 0 °C and 20 min at room temperature. The mixture was concentrated in vacuo, and the residue was purified by flash column chromatography on silica gel (hexane) to afford crude (2-bromoethyl)-di-*tert*-butylsilane. Crude (2-bromoethyl)di-*tert*-butylsilane and sodium azide (105 mg, 1.61 mmol) were dissolved in DMF (3.4 mL) and stirred at room temperature for 6 h. The reaction was diluted with EtOAc and washed with brine (2 \times), and the organic phase was dried over MgSO₄ and concentrated. The residue was purified by flash column chromatography on silica gel (hexane) to obtain **26** (130 mg, 57% over two steps) as colorless liquid. *R*_f 0.35 (hexane). ¹H NMR (400 MHz, CDCl₃) δ 3.41–3.37 (m, 2H, CH₂N₃), 3.31 (t, *J* = 2.5 Hz, 1H, SiH), 1.08–1.05 (m, 2H, SiCH₂), 1.03 (s, 18H, CH₃). IR (neat) 2931, 2887, 2858, 2087, 1468, 1244 cm^{-1} .

2-Amino-3-(1-(2-(Di-*tert*-butylsilyl)ethyl)-1H-1,2,3-triazol-4-yl)propanoic Acid (27). Azide **26** (140 mg, 0.66 mmol), propargyl glycine (75 mg, 0.66 mmol), copper(II) acetate (12 mg, 0.07 mmol), and (+)-sodium L-ascorbate (130 mg, 0.66 mmol) were dissolved in *n*-BuOH (3.3 mL) and water (3.3 mL). The reaction was stirred at room

temperature overnight and concentrated in vacuo. The residue was purified by flash column chromatography on silica gel (9:1 \rightarrow 4:1, *n*-BuOH/AcOH) to obtain **27** (47 mg, 22%) as white solid. ¹H NMR (400 MHz, C₂D₆O₅) δ 8.01 (s, 1H, CHN), 4.45–4.40 (m, 2H, CH₂N), 3.86 (s, 1H, CHCH₂), 3.23–3.02 (m, 2H, CH₂CH), 1.31–1.24 (m, 2H, SiCH₂), 1.03 (s, 18H, CH₃). ²⁹Si NMR (CDCl₃, 99 MHz) δ 10.1. HRMS (ESI) calcd for [C₁₅H₃₁N₄O₂Si]⁺, 327.2211; found, 327.2200.

2-(Di-*tert*-butylsilyl)acetic Acid (28). To a solution of **25** (750 mg, 4 mmol) in DCM (52 mL), PCC (1.32 g, 6 mmol) was added and the mixture was stirred at room temperature for 3 h. The reaction mixture was diluted with diethyl ether and filtered through Celite (diethyl ether). The residue was concentrated in vacuo, redissolved in acetone (40 mL), and cooled to 0 °C. A solution of sodium chlorite (1.36 g, 12 mmol) and sulfamic acid (1.09 g, 11.2 mmol) in water (40 mL) was added dropwise, and the mixture was stirred at 0 °C. After 30 min, the reaction was diluted with water and extracted with EtOAc (4 \times). The organic phases were combined, dried over MgSO₄, and concentrated in vacuo. The residue was purified by flash column chromatography on Reprospher Acidosil-S, 50 μm (hexane), to yield **28** (209 mg, 26% over two steps) as colorless solid. *R*_f 0.24 (1:9, EtOAc/hexane). ¹H NMR (CDCl₃, 400 MHz) δ 3.59 (t, *J* = 2.9 Hz, 1H, SiH), 1.99 (d, *J* = 3.0 Hz, 2H, CH₂), 1.06 (s, 18H, CH₃). ¹³C NMR (CDCl₃, 100 MHz) δ 180.4, 28.3, 19.2, 18.9. ²⁹Si NMR (CDCl₃, 99 MHz) δ 11.3. IR (neat): 2932, 2890, 2859, 2118, 1690, 1469, 1422, 1390, 1367, 1289, 1146, 1109, 1013 cm^{-1} . HRMS (ESI) calcd for [C₁₀H₂₃O₂Si]⁻, 201.1316; found, 201.1318.

***N*-Benzyl-2-(di-*tert*-butylsilyl)acetamide (29).** To a solution of **28** (51 mg, 0.25 mmol) in THF (2.5 mL), DIPEA (0.11 mL, 0.63 mmol) and benzylamine (0.03 mL, 0.25 mmol) were added and the mixture was cooled to 0 °C. T3P as a 50% solution in THF (1.2 mL, 2 mmol) was added dropwise, and the mixture was stirred at 0 °C for 30 min, warmed to room temperature, and stirred overnight. The reaction was diluted with EtOAc and washed with water (1 \times) and brine (1 \times). After drying over MgSO₄, the organic phase was concentrated in vacuo. The residue was purified by flash column chromatography on silica gel (9:1 \rightarrow 4:1, hexane/EtOAc) to afford **29** (26 mg, 35%) as white crystals. *R*_f 0.27 (4:1, hexane/EtOAc). ¹H NMR (CDCl₃, 400 MHz) δ 7.24–7.36 (m, 5H, Ar-H), 5.61 (s, 1H, NH), 4.41 (d, *J* = 5.7 Hz, 2H, NHCH₂), 3.59 (t, *J* = 3.3 Hz, 1H, SiH), 1.90 (d, *J* = 3.5 Hz, 2H, SiCH₂), 1.05 (s, 18H, CH₃). ¹³C NMR (CDCl₃, 100 MHz) δ 138.5, 128.6, 127.9, 127.4, 44.0, 28.5, 21.0, 19.0. ²⁹Si NMR (CDCl₃, 99 MHz) δ 11.4. IR (neat): 3291, 2929, 2886, 2857, 2111, 1630, 1542, 1497, 1469, 1455, 1364, 1291, 1261, 1155, 1131, 1012 cm^{-1} . HRMS (ESI) calcd for [C₁₇H₃₀NOSi]⁺, 292.2091; found, 292.2094.

***N*-Benzyl-2-(di-*tert*-butylfluorosilyl)acetamide (8).** To a mixture of di-*tert*-butylfluorosilane (**30**, 228 mg, 1.40 mmol; see ref 32 for its preparation) in DCM (0.7 mL) was added rhodium(II) acetate dimer (3.10 mg, 7 μmol) followed by dropwise addition of *N*-benzyl-2-diazoacetamide (**31**, 123 mg, 0.702 mmol; see ref 33 for its preparation) in DCM (1.2 mL). The reaction was stirred at room temperature for 15 min, filtered through Celite (DCM), and concentrated in vacuo. The residue was purified by flash column chromatography (9:1 \rightarrow 4:1, hexane/EtOAc) to afford **8** (11 mg, 5%) as colorless solid. *R*_f 0.44 (7:3, hexane/EtOAc). ¹H NMR (CDCl₃, 400 MHz) δ 7.36–7.25 (m, 5H, Ar-H), 5.71 (s, 1H, NH), 4.42 (d, *J* = 5.4 Hz, 2H, NHCH₂), 2.03 (d, *J* = 2.0 Hz, 2H, SiCH₂), 1.07 (d, *J* = 1.0 Hz, 18H, CH₃). ¹³C NMR (CDCl₃, 100 MHz) δ 138.3, 128.7, 127.9, 127.6, 44.1, 27.0, 20.3, 20.1. ¹⁹F NMR (CDCl₃, 376 MHz) δ -181.2. HRMS (ESI) calcd for [C₁₇H₂₉FNOSi]⁺, 310.1997; found, 310.1992.

The NMR tube containing the sample was stored at room temperature for 7 d and was then analyzed again by ¹H NMR and ¹⁹F NMR spectroscopy. ¹H NMR (CDCl₃, 400 MHz) δ 7.36–7.28 (m, 5H), 5.70 (br s, 1H), 4.44 (d, *J* = 5.7 Hz, 2H), 2.03 (s, 3H), 1.06 (d, *J* = 1.0 Hz, 18H). ¹⁹F NMR (CDCl₃, 376 MHz) δ -157.7. The observed chemical shifts point to decomposition products **32** and **33**. For verification, compounds **32** and **33** were separately synthesized.

Di-*tert*-butylfluorosilanol (32). **32** was synthesized in analogy to a published procedure.³⁴ Briefly, dichloro-di-*tert*-butylsilane was reacted with trifluorostibine to obtain di-*tert*-butyldifluorosilane. Further treatment with KOH afforded **32**. ¹H NMR (CDCl₃, 400 MHz) δ 1.06 (d, *J* = 1.0 Hz, 18H, CH₃). ¹⁹F NMR (CDCl₃, 376 MHz) δ -157.6.

N-Benzylacetamide (33). To a solution of benzylamine (0.5 mL, 4.58 mmol) in DCM (17.0 mL) was added triethylamine (1.28 mL, 9.16 mmol) and 4-(dimethylamino)pyridine (0.056 g, 0.458 mmol) at 0 °C. Acetic anhydride (0.432 mL, 4.58 mmol) was added dropwise, and the mixture was stirred for 10 min at 0 °C and 30 min at room temperature. The reaction was washed with saturated aqueous NaHCO₃ (1×), 1 M HCl (1×), water (1×), and brine (1×). The organic phase was concentrated in vacuo to obtain **33** (670 mg, 97%) as white solid. ¹H NMR (CDCl₃, 400 MHz) δ 7.38–7.28 (m, 5H, Ar-H), 6.05 (br s, 1H, NH), 4.44 (d, J = 5.8, 2H, CH₂), 2.03 (s, 3H, CH₃).

tert-Butyl 4-Bromophenethylcarbamate (35). To a solution of 4-bromophenethylamine (**34**, 6.94 g, 34 mmol) in CH₃OH (100 mL) was added NEt₃ (19 mL, 136 mmol) and di-*tert*-butyl dicarbonate (15.3 g, 68 mmol) at 0 °C. The mixture was stirred at room temperature for 14 h. The reaction was concentrated, diluted with EtOAc, and washed with water (2×) and brine (1×). After drying over MgSO₄, concentration of the organic phase in vacuo afforded a residue, which was further purified by flash column chromatography on silica gel (19:1 → 17:5, hexane/EtOAc) to afford **35** (10.2 g, quantitative) as white solid. R_f 0.34 (4:1, hexane/EtOAc). ¹H NMR (400 MHz, CDCl₃) δ = 7.43–7.40 (m, 2H), 7.06 (d, J = 8.4 Hz, 2H), 4.54 (s, 1H), 3.36–3.32 (m, 2H), 2.75 (t, J = 7.0 Hz, 2H), 1.43 (s, 9H). ¹³C NMR (100 MHz, CDCl₃) δ = 155.8, 138.0, 131.6, 130.5, 120.2, 79.3, 41.6, 35.7, 28.4. IR (neat) 3444, 3355, 2977, 2932, 2871, 1694, 1488, 1365, 1248, 1164 cm⁻¹. HRMS (ESI) calcd for [C₁₃H₁₈BrNNaO₂]⁺, 322.0413; found, 322.0414.

2,3-Diacetoxy-4-(4-(di-*tert*-butylsilyl)phenethylamino)-4-oxobutanoic Acid (36). *n*-BuLi (6.18 mL, 9.89 mmol) was added dropwise to a solution of **35** (990 mg, 3.3 mmol) in THF (11 mL) at –78 °C. The colorless mixture was stirred at –78 °C and after 1.5 h was treated with di-*tert*-butylchlorosilane (1.04 mL, 4.95 mmol). After warming to room temperature, the reaction mixture was further stirred for 20 h and the resulting yellow mixture was poured into 0.3 M aqueous NaHCO₃ solution and extracted with EtOAc (3×). The combined organic phases were washed with water (1×) and brine (1×), dried over MgSO₄, and concentrated in vacuo. A 1.25 M HCl/CH₃OH solution (5 mL) was added to the residue, and the mixture was stirred at room temperature for 1 h. After concentration in vacuo, the resulting solid was mixed with acetonitrile (CH₃CN, 16.5 mL) and dissolved by adding NEt₃ (0.15 mL, 1.07 mmol). Cobalt(II) chloride (21 mg, 0.17 mmol) and di-*O*-acetyl-tartaric acid anhydride (1.07 g, 4.95 mmol) were added, and the blue solution was stirred at room temperature for 5 h. The reaction mixture was poured into 1 M HCl solution and extracted with EtOAc (2×). The combined organic phases were poured into 0.3 M aqueous NaHCO₃ and extracted with EtOAc (3×). After drying over MgSO₄, the combined organic phases were concentrated in vacuo. The residue was purified by flash column chromatography on Reprospher Acidosil-S, 50 μm (9:1 → 4:1, hexane/EtOAc), to yield **36** (338 mg, 21% over three steps) as colorless foam. R_f 0.26 (75:27:5:0.5, CHCl₃/CH₃OH/H₂O/AcOH). ¹H NMR (CDCl₃, 400 MHz) δ 7.48 (d, J = 7.5 Hz, 2H), 7.15 (d, J = 7.3 Hz, 2H), 7.07 (s, 1H), 5.76 (s, 1H), 5.54 (s, 1H), 3.83 (s, 1H), 3.50 (s, 2H), 2.78 (s, 2H), 2.06 (s, 6H), 1.02 (s, 18H). ¹³C NMR (CDCl₃, 100 MHz) δ 170.1, 167.1, 139.3, 136.1, 133.4, 128.6, 127.9, 72.7, 40.7, 35.4, 35.2, 33.7, 28.9, 22.3, 20.6, 20.5, 19.0, 13.9. ²⁹Si NMR (CDCl₃, 99 MHz) δ 12.9 (J_{Si-H} = 186 Hz). IR (neat) 3358, 2931, 2856, 2097, 1749, 1631, 1544, 1413, 1372, 1212, 1055, 803 cm⁻¹. HRMS (ESI) calcd for [C₂₄H₃₆NNa₂O₇Si]⁺, 524.2051; found, 524.2055.

2,3-Diacetoxy-4-(4-(di-*tert*-butylfluorosilyl)phenethylamino)-4-oxobutanoic Acid (37). To a solution of **36** (200 mg, 0.42 mmol) in THF (4.2 mL), AcOH (72 μL, 1.25 mmol), K222 (235 mg, 0.63 mmol), and potassium fluoride (37 mg, 0.625 mmol) were added and the reaction mixture was heated under reflux for 6 h. Thereafter, the yellow mixture was washed with saturated aqueous NH₄Cl solution (1×), water (1×), and brine (1×), and the organic phase was dried over MgSO₄ and concentrated in vacuo. Purification of the residue was accomplished by flash column chromatography on Reprospher Acidosil-S, 50 μm (9:1 → 4:1, hexane/EtOAc), to yield **37** (74 mg, 36%) as white–yellow solid. R_f 0.10 (90:10:1:0.5, CHCl₃/CH₃OH/H₂O/AcOH). ¹H NMR (CDCl₃, 400 MHz) δ 7.54 (d, J = 7.8 Hz, 2H, Ar-H), 7.20 (d, J = 8.0 Hz, 2H, Ar-H), 6.65 (s, 1H, NH), 5.79 (s, 1H, CH), 5.60 (s, 1H, CH), 3.50–3.47 (m, 2H, CH₂N), 2.81 (t, J = 7.2 Hz, 2H, CH₂-Ar), 2.08 (s, 6H,

C(O)CH₃), 1.04 (s, 18H, C(CH₃)₃). ¹³C NMR (CDCl₃, 100 MHz) δ 170.0, 166.6, 139.8, 134.4, 134.3, 131.8, 131.7, 128.7, 128.6, 128.1, 72.2, 40.6, 35.5, 33.7, 29.7, 28.9, 27.3, 22.3, 20.5, 20.4, 20.3, 20.2, 13.9. ¹⁹F NMR (CDCl₃, 376 MHz) δ –188.9. IR (neat) 3362, 2935, 2893, 2860, 1751, 1659, 1539, 1372, 1209, 1109, 1060 cm⁻¹. HRMS (ESI) calcd for [C₂₄H₃₇FNO₇Si]⁺, 498.2318; found, 498.2305.

Peptide Synthesis. Fmoc deprotection (general procedure): The resin-bound Fmoc peptide was treated with 20% piperidine in DMF (v/v) for 5 min. This step was repeated with a reaction time of 20 min. The resin was washed with DMF (2×), DCM (2×), and DMF (2×).

HBTU/HOBT coupling (general procedure): A solution of Fmoc-Xaa-OH (Xaa = amino acid, 4 equiv), HBTU (4 equiv), HOBT (4 equiv), and DIPEA (4 equiv) in DMF was added to the resin-bound, free amine peptide and shaken for 90 min at room temperature. This step was repeated with a reaction time of 60 min. The resin was washed with DMF (2×), DCM (2×), and DMF (2×). The peptides were typically prepared starting with 147 mg (100 μmol) of the resin. The amounts of reagents and building blocks in all subsequent reactions were calculated based on this amount.

Synthesis of 2-(4-(Di-*tert*-butylfluorosilyl)phenyl)acetyl-Ala-(SO₃H)-Ala(SO₃H)-Ava-Gln-Trp-Ala-Val-NMeGly-His-Sta-Leu-NH₂ (Precursor Compound 38). The resin-bound, side chain protected peptide was prepared according to the general procedures described above. 2-(4-(Di-*tert*-butylsilyl)phenyl)acetic acid (100 mg, 359 μmol) and HBTU (136.2 mg, 359 μmol) were dissolved in DMF (5 mL), and DIPEA (63 μL, 359 μmol) was added. The resin-bound peptide (179 μmol) was suspended in this solution, and the suspension was shaken for 24 h at room temperature. The resin was then filtered, washed with DMF (5 × 5 mL) and DCM (5 × 5 mL), and dried in vacuo. Subsequent treatment of the resin with 2 mL of TFA/water/triisopropylsilane/phenol (85:5:5:5) afforded the crude, fully deprotected peptide, which was precipitated and washed with cold methyl *tert*-butyl ether. The crude peptide was dried in vacuo, purified by preparative reversed phase (RP) HPLC, and lyophilized to afford **38** (30 mg, 9.6%) as white solid. The product was analyzed by HPLC-MS: *m/z* calcd, 1641.8; found, 1642.0 ([M + H]⁺).

Synthesis of 2-(4-(Di-*tert*-butylfluorosilyl)phenyl)acetyl-Ala-(SO₃H)-Ala(SO₃H)-Ava-Gln-Trp-Ala-Val-NMeGly-His-Sta-Leu-NH₂ (Reference Compound 39). **38** (9.3 mg, 5.7 μmol) was dissolved in THF (1 mL). The solution was added to a mixture of KF (2.6 mg, 45.3 μmol), K222 (17.1 mg, 45.3 μmol), and K₂CO₃ (3.1 mg, 22.7 μmol). Glacial acetic acid (7.8 μL, 135.9 μmol) was added, and the resulting suspension was heated at 70 °C for 30 min. The crude mixture was directly subjected to preparative RP-HPLC, and the purified product was lyophilized to obtain **39** (6 mg, 58%) as white solid. The product was analyzed by HPLC-MS: *m/z* calcd, 1659.8; found, 1660.4 ([M + H]⁺).

Procedure for the Syntheses of 4-((4-(Di-*tert*-butylsilyl)phenethylamino)-2,3-dihydroxy-4-oxobutanoyl-Arg-Ava-Gln-Trp-Ala-Val-NMeGly-His-Sta-Leu-NH₂ and 4-((4-(Di-*tert*-butylsilyl)phenethylamino)-2,3-dihydroxy-4-oxobutanoyl-Ala(SO₃H)-Ala(SO₃H)-Ava-Gln-Trp-Ala-Val-NMeGly-His-Sta-Leu-NH₂ (Precursor Compounds 40 and 42). The resin-bound, side chain protected peptide was prepared according to the general procedures described above. **36** (165.0 mg, 344 μmol), DMTMM-BF₄ (120.4 mg, 367 μmol), and NMM (69.6 μL, 688 μmol) were dissolved in DMF (10 mL). The resin-bound peptide (230 μmol) was suspended in this solution, and the suspension was shaken for 30 min at ambient temperature. Thereafter the resin was filtered and washed with DMF (3 × 10 mL) and then treated with hydrazine monohydrate (1.1 mL) in DMF (5 mL) at room temperature for 3 h to remove the acetyl groups, washed with DMF (3 × 5 mL) and DCM (3 × 5 mL), and dried in vacuo. Subsequent treatment of the resin with 2.5 mL TFA/water/triisopropylsilane/phenol (85:5:5:5) afforded the crude, fully deprotected peptide, which was precipitated and washed with cold methyl *tert*-butyl ether. The crude peptide was dried in vacuo, purified by preparative RP-HPLC, and lyophilized. The products were analyzed by HPLC-MS: **40** (5.7 mg, 1.5%) as white solid; *m/z* calcd, 807.0; found, 807.2 ([M + 2H]²⁺). **42** (11.5 mg, 1.8%) as white solid; *m/z* calcd, 1759.8; found, 1760.7 ([M + H]⁺).

Synthesis of 4-((4-(Di-*tert*-butylfluorosilyl)phenethylamino)-2,3-dihydroxy-4-oxobutanoyl-Arg-Ava-Gln-Trp-Ala-Val-NMeGly-His-Sta-Leu-NH₂ and 4-((4-(Di-*tert*-butylfluorosilyl)phenethylamino)-2,3-dihydroxy-4-oxobutanoyl-Ala(SO₃H)-Ala(SO₃H)-Ava-Gln-Trp-Ala-Val-NMeGly-His-Sta-Leu-NH₂ (Reference Compounds 41 and 43). The resin-bound, side

chain protected peptide was prepared according to the general procedures described above. **37** (22.4 mg, 45 μmol), DMTMM-BF₄ (15.7 mg, 48 μmol), and NMM (10 μL , 90 μmol) were dissolved in DMF (2 mL). The resin-bound peptide (30 μmol) was suspended in this solution, and the suspension was shaken for 12 h at ambient temperature. The resin was then filtered and washed with DMF (3 \times 3 mL). The resin was treated with hydrazine monohydrate (0.1 mL) in DMF (0.9 mL) at room temperature for 6 h to remove the acetyl groups, washed with DMF (3 \times 5 mL) and DCM (3 \times 5 mL), and dried in vacuo. Subsequent treatment of the resin with 2 mL of TFA/water/triisopropylsilane/phenol (85:5:5:5) afforded the crude, fully deprotected peptide, which was precipitated and washed with cold methyl *tert*-butyl ether. The crude peptide was dried in vacuo, purified by preparative RP-HPLC, and lyophilized. The products were analyzed by HPLC-MS: **41** (2.4 mg, 3.1%) as white solid; *m/z* calcd, 816.0; found, 816.2 ($[(M + 2H)/2]^+$). **43** (3.8 mg, 3.6%) as white solid; *m/z* calcd, 1776.8; found, 1777.7 ($[M + H]^+$).

In Vitro Receptor Binding Assay. The binding affinity of the nonradioactive bombesin peptides **39** and **41** for human GRPr was determined in a displacement assay with PC-3 cells (DSMZ, German Collection of Microorganisms and Cell Cultures). Cells were seeded in 48-well plates (8 \times 10⁴ cells/well) and grown in Ham's F-12 nutrient mix with GlutaMax (Invitrogen) for 1 day to subconfluence. Cells were washed twice with PBS, followed by the addition of incubation buffer. The test compound was dissolved in DMSO to produce 1 mM stock solutions and further diluted in incubation buffer (50 mM 2-(4-(2-hydroxyethyl)-1-piperazine)ethanesulfonic acid (HEPES), protease inhibitor complete (1 tablet/50 mL; Roche Diagnostics GmbH), 5 mM MgCl₂, and 0.1% BSA (pH 7.4) in Dulbecco Modified Eagle Medium with GlutaMAX I (Invitrogen)) to 10⁻¹⁰–10⁻³ M. Test compound solutions and [¹²⁵I]-Tyr⁴-bombesin (PerkinElmer; specific radioactivity, 81.4 GBq/ μmol ; conc, 22.73 nM; K_D = 0.81 nM) were added to all well plates (final volume, 960 μL ; test compound concentration range, 10⁻⁵–10⁻¹² M; [¹²⁵I]-Tyr⁴-bombesin concentration, 0.237 nM). Nonspecific binding was estimated with Tyr⁴-bombesin (concentration per well: 1.0 μM). After incubation at room temperature for 1 h, cells were washed twice with cold PBS (containing 0.1% BSA) and solubilized with 0.25% trypsin ethylenediaminetetraacetic acid solution (0.3 mL/well, incubation for 15 min at 37 °C). Cells were pipetted into Eppendorf cups, and wells were washed with PBS (1 mL) and added to cell solutions. Radioactivity was measured in a γ -counter (1480 Wizard, PerkinElmer). The IC₅₀ values were calculated using KELL Radlig software (Biosoft).

Radiolabeling. No-carrier-added aqueous [¹⁸F]fluoride ion was produced on an IBA Cyclone 18/9 cyclotron by irradiation of 98% enriched [¹⁸O]H₂O (2.0 mL) using an 18-MeV proton beam via the [¹⁸O(p,n)¹⁸F] nuclear reaction. [¹⁸F]Fluoride was trapped on an anion-exchange resin cartridge (Sep-Pak QMA Light, Waters; preconditioning with 0.5 M K₂CO₃ solution (5 mL), water (10 mL), and air (10 mL)). The cartridge was eluted with a solution of K222 (5.0 mg) and potassium carbonate (1.0 mg) in H₂O (0.3 mL) and CH₃CN (1.2 mL). Solvents were removed by heating at 95 °C for 20 min, applying a gentle stream of nitrogen. During this time, CH₃CN (3 \times 1 mL) was added and evaporated to give the dry K[¹⁸F]F/K222 complex. After the radiolabeling reaction, the identity of the ¹⁸F-labeled products was confirmed by comparison with the HPLC retention time of their nonradioactive reference compounds or by coinjection using analytical radio-HPLC (gradient CH₃CN/H₂O + 0.1% TFA 5:95–95:5 in 20 min, 1.0 mL/min). For the analysis of crude reaction mixture, an ultraperformance liquid chromatography (UPLC, Waters) system with an Acquity UPLC BEH C18 column (2.1 mm \times 50 mm, 1.7 μm , Waters) and an attached coincidence detector (FlowStar LB513, Berthold) was used (gradient CH₃CN/H₂O + 0.1% TFA 5:95 \rightarrow 95:5 in 4 min, 0.6 mL/min).

2-(Di-*tert*-butyl[¹⁸F]fluorosilyl)ethanol ([¹⁸F]2**).** A solution of **25** (2.0 mg) and glacial acetic acid (10 μL) in anhydrous DMSO (150 μL) was added to the dry K[¹⁸F]F/K222 complex and heated at 110 °C for 20 min. An aliquot of the crude reaction mixture was analyzed using an analytical UPLC to show an ¹⁸F-incorporation of $\geq 95\%$.

2-Amino-3-(1-(2-(di-*tert*-butyl[¹⁸F]fluorosilyl)ethyl)-1H-1,2,3-triazol-4-yl)propanoic Acid ([¹⁸F]18**).** A solution of **27** (2.0 mg) and glacial

acetic acid (10 μL) in anhydrous DMSO (150 μL) was added to the dry K[¹⁸F]F/K222 complex and heated at 110 °C for 20 min. An aliquot of the crude reaction mixture was analyzed using an analytical UPLC to show an ¹⁸F-incorporation of $\geq 95\%$.

***N*-Benzyl-2-(di-*tert*-butyl[¹⁸F]fluorosilyl)acetamide ([¹⁸F]**8**).** A solution of **29** (2.0 mg) and glacial acetic acid (10 μL) in anhydrous DMSO (150 μL) was added to the dry K[¹⁸F]F/K222 complex and heated at 110 °C for 20 min. An aliquot of the crude reaction mixture was analyzed using an analytical UPLC to show an ¹⁸F-incorporation of $\geq 95\%$. TLC analysis (9:1, hexane/EtOAc) of the crude reaction mixture showed that the ¹⁸F-labeled product did not correspond to compound **8** but rather to **32**.

2-(4-(Di-*tert*-butyl[¹⁸F]fluorosilyl)phenyl)acetyl-Ala(SO₃H)-Ala(SO₃H)-Ava-Gln-Trp-Ala-Val-NMeGly-His-Sta-Leu-NH₂ ([¹⁸F]39**).** A solution of **38** (2.0 mg) and glacial acetic acid (10 μL) in anhydrous DMSO (150 μL) was added to the dry K[¹⁸F]F/K222 complex and heated at 110 °C for 20 min. An aliquot of the crude reaction mixture was analyzed using an analytical HPLC (ACE C18, 50 mm \times 4.6 mm, 5 μm ; gradient CH₃CN/H₂O + 0.1% TFA 5:95 \rightarrow 95:5 in 20 min, 1.0 mL/min) before addition of H₂O/CH₃CN (9:1, 2 mL) into the reaction vial. The diluted reaction mixture was injected into a semipreparative HPLC (ACE C18, 250 mm \times 10 mm, 5 μm ; isocratic CH₃CN/H₂O + 0.1% TFA 37:63, 4.0 mL/min), and the product peak was collected. The product fraction was diluted with water (20 mL) and immobilized on a C18 cartridge (Sep-Pak Light C18, Waters, or Chromafix C18 (s), Machery-Nagel). After washing with water (20 mL), [¹⁸F]**39** was eluted with ethanol (1 mL). The solvent was evaporated at 90 °C. For in vivo applications, [¹⁸F]**39** was reconstituted in 0.15 M PBS containing $\leq 5\%$ ethanol (v/v) and the solution was filtered sterile. The overall synthesis time was 80 min. Reverse-phase HPLC revealed a radiochemical purity $\geq 95\%$. The synthesis afforded 350 MBq of [¹⁸F]**39** starting from 32.05 GBq of the dried K[¹⁸F]F/K222 complex. The product could be obtained in specific radioactivity of 35 GBq/ μmol and radiochemical yield (RCY) of 1.8% (decay corrected) and was stable in PBS over 2 h.

4-((4-(Di-*tert*-butylfluorosilyl)phenethyl)amino)-2,3-dihydroxy-4-oxobutanoyl-Ala(SO₃H)-Ala(SO₃H)-Ava-Gln-Trp-Ala-Val-NMeGly-His-Sta-Leu-NH₂ ([¹⁸F]43**).** A solution of **42** (2.0 mg) and glacial acetic acid (10 μL) in anhydrous DMSO (150 μL) was added to the dry K[¹⁸F]F/K222 complex and heated at 110 °C for 20 min. An aliquot of the crude reaction mixture was analyzed using an analytical HPLC (ACE C18, 50 mm \times 4.6 mm, 5 μm ; gradient CH₃CN/H₂O + 0.1% TFA 5:95 \rightarrow 95:5 in 20 min, 1.0 mL/min) before addition of H₂O/CH₃CN (9:1, 2 mL) into the reaction vial. The diluted reaction mixture was injected into a semipreparative HPLC (ACE C18, 250 mm \times 10 mm, 5 μm ; isocratic CH₃CN/H₂O + 0.1% TFA 40:60, 4.0 mL/min), and the product peak was collected. The product fraction was diluted with water (20 mL) and immobilized on a C18 cartridge (Sep-Pak light C18, Waters, or Chromafix C18 (s), Machery-Nagel). After washing with water (20 mL), [¹⁸F]**43** was eluted with ethanol (1 mL). The solvent was evaporated at 90 °C. For in vivo applications, [¹⁸F]**43** was reconstituted in 0.15 M PBS containing $\leq 5\%$ ethanol (v/v), and the solution was filtered sterile. The overall synthesis time was 80 min. Reverse-phase HPLC revealed a radiochemical purity $\geq 90\%$. The synthesis afforded 190 MBq of [¹⁸F]**43** starting from 29.68 GBq of the dried K[¹⁸F]F/K222 complex. The product could be obtained in specific radioactivity of 70 GBq/ μmol and RCY of 1.1% (decay corrected) and was stable in PBS over 2 h.

Hydrolytic Stability of the Si–¹⁸F Bond. The reaction mixture containing [¹⁸F]**2** or [¹⁸F]**18** was diluted in water (2.0 mL) and passed through on a C18 cartridge (Sep-Pak light C18, Waters, or Chromafix C18 (s), Machery-Nagel). After washing with water (5.0 mL), [¹⁸F]**2** or [¹⁸F]**18** was eluted with ethanol (1.0 mL) and aliquots were diluted in either water, 0.9% NaCl, or 0.15 M PBS. Analysis was performed at various time points (30, 50, 75, 80, 100, 210 min) using an UPLC (Waters) system with an Acquity UPLC BEH C18 column (2.1 mm \times 50 mm, 1.7 μm , Waters) and an attached coincidence detector (FlowStar LB513, Berthold, gradient CH₃CN/H₂O + 0.1% TFA 5:95 \rightarrow 95:5 in 4 min, 0.6 mL/min). The hydrolysis of [¹⁸F]**2** or [¹⁸F]**18** was followed by formation of corresponding amounts of ¹⁸F. The half-lives

were derived from the linear function of time and the amount of intact labeled compound.

log $D_{7.4}$ Measurement. The determination of log $D_{7.4}$ was carried out in analogy to a published procedure.³⁵ Briefly, [^{18}F]39 was added to a mixture of PBS (0.5 mL, pH = 7.4) and 1-octanol (0.5 mL) at room temperature. The mixture was equilibrated for 15 min in an overhead shaker and further centrifuged (3 min, 5000 rpm). Aliquots (50 μL) of each of two phases were analyzed in a γ -counter. The partition coefficient is expressed as the ratio between the radioactivity concentrations (cpm/mL) of the 1-octanol and PBS phase. Values represent the mean \pm standard deviation of three determinations from one experiment.

Animals. Animal studies complied with Swiss laws on animal protection and husbandry and were approved by the Veterinary office of the Canton Zurich. After an acclimatization period, tumor xenografts were produced in 6-week-old male NMRI nude mice (Charles River) by subcutaneous injection in the right shoulder region of 5×10^6 PC-3 cells in 100 μL of PBS (pH 7.4) under 2–3% isoflurane anesthesia. PET and ex vivo biodistribution experiments were conducted when the xenografts reached a volume of about 1 cm^3 .

Small Animal PET. Xenograft-bearing animals (33–35 g, $n = 3$) were injected via tail vein with [^{18}F]39 (8.3–15.3 MBq in 100–150 μL of PBS containing $\leq 5\%$ ethanol, 390–630 pmol). To determine specific binding, an additional group of mice (32–34 g, $n = 3$) received 50 μg of nonradioactive bombesin coinjected with [^{18}F]39 (4.8–10.5 MBq in 110–150 μL of PBS containing $\leq 5\%$ ethanol, 510–575 pmol). In a preliminary study, xenograft-bearing animals (30 and 32 g) were administered [^{18}F]43 (5.1 MBq in 100 μL of PBS containing $\leq 5\%$ ethanol, 93 pmol, $n = 1$ or 3.6 MBq in 100 μL PBS containing $\leq 5\%$ ethanol, 96 pmol, and $n = 1$). Anesthesia was induced with 5% isoflurane (Abbott) in O_2/air 10 min before PET acquisition. Depth of anesthesia and body temperature were controlled as described by Honer et al.³⁶ PET scans were performed under 2–3% isoflurane anesthesia with a GE VISTA eXplore PET/CT tomograph. Static scans in two bed positions (15 min upper body followed by 15 min lower body) with [^{18}F]39 were carried out 60–105 min after injection. Dynamic scans with [^{18}F]43 were acquired in one bed position (list mode) from 2 to 92 min or from 80 to 170 min after tracer injection. Data were reconstructed by two-dimensional ordered-subset expectation maximization (2D OSEM); dynamic scans were reconstructed into 5 min time frames. Region of interest analysis was conducted with the PMOD 3.3 software (PMOD, Switzerland). Standardized uptake values (SUV) were calculated as a ratio of tissue radioactivity concentration (kBq/cm^3) and injected activity dose per gram body weight (kBq/g), both decay-corrected.

Ex Vivo Biodistribution. Animals used for PET imaging were subsequently sacrificed for ex vivo biodistribution (see section above for amount of radioactivity injected). Animals ($n = 6$) injected with [^{18}F]39 were sacrificed at 117 min after injection. Animals, which were administered with [^{18}F]43, were sacrificed at 104 min ($n = 1$) or 182 min ($n = 1$) after injection. Organs and tissues of interest were collected and weighed, and the amount of radioactivity was determined in a γ -counter to calculate percentage uptake (% injected dose per gram of tissue).

■ ASSOCIATED CONTENT

● Supporting Information

HPLC chromatograms of the quality control of compounds ^{18}F -39 and ^{18}F -43 as well as the chromatograms of the radiofluorination reaction mixture with 29 coinjected with precursor 29 and reference 8. This material is available free of charge via the Internet at <http://pubs.acs.org>.

■ AUTHOR INFORMATION

Corresponding Author

*Phone: +41 44 633 74 63. Fax: +41 44 633 13 67. E-mail: simon.ametamey@pharma.ethz.ch. Address: Center for Radiopharmaceutical Sciences of ETH, PSI and USZ, Department of Chemistry and Applied Biosciences, ETH Hönggerberg, Wolfgang-Pauli-Strasse 10, CH-8093 Zurich, Switzerland.

Present Address

^{||}L.M.D.: Piramal Imaging, Tegelerstrasse 6-7, 13353 Berlin, Germany.

Author Contributions

All authors have given approval to the final version of the manuscript.

Notes

The authors declare no competing financial interest.

■ ACKNOWLEDGMENTS

We gratefully acknowledge Claudia Keller, Peter Friese, Katrin Dinse, Dr. Thomas Nauser, and Mathias Nobst for their experimental assistance and technical support. We also thank Dr. Steven Donald for carrying out some of the early calculations on selected compounds.

■ ABBREVIATIONS USED

AcOH, acetic acid; β^+ , positron; C–F, carbon–fluorine; CH_3CN , acetonitrile; CuAAC, copper-catalyzed azide–alkyne cycloaddition; DFT, density functional theory; DIPEA, *N,N*-diisopropylethylamine; DMTMM-BF₄, 4-(4,6-dimethoxy-1,3,5-triazin-2-yl)-4-methylmorpholinium tetrafluoroborate; EOS, end of synthesis; EtOAc, ethylacetate; ^{18}F , fluorine-18; GBq, gigabecquerel; GRPr, gastrin-releasing peptide receptor; HBTU, *O*-(benzotriazol-1-yl)-*N,N,N,N*-tetramethyluronium hexafluorophosphate; HOBT, 1-hydroxybenzotriazole; KF, potassium fluoride; K222, Kryptofix 222; log $D_{7.4}$, logarithmic distribution coefficient; MBq, megabecquerel; *n*-BuLi, *n*-butyllithium; NMM, *N*-methylmorpholine; OH^- , hydroxide anion; pi, postinjection; PC-3, human prostate adenocarcinoma; PET, positron emission tomography; RP, reversed phase; Si–CH₂, silicon–methylene; Si–F, silicon–fluorine; SENs, shared electron numbers; SUV, standardized uptake values; T3P, 2,4,6-tripropyl-1,3,5,2,4,6-trioxatrimphosphorinane 2,4,6-trioxide; UPLC, ultraperformance liquid chromatography

■ REFERENCES

- (1) Blok, D.; Feitsma, R. I.; Vermeij, P.; Pauwels, E. J. Peptide radiopharmaceuticals in nuclear medicine. *Eur. J. Nucl. Med.* **1999**, *26*, 1511–1519.
- (2) McAfee, J. G.; Neumann, R. D. Radiolabeled peptides and other ligands for receptors overexpressed in tumor cells for imaging neoplasms. *Nucl. Med. Biol.* **1996**, *23*, 673–676.
- (3) Okarvi, S. M. Peptide-based radiopharmaceuticals: future tools for diagnostic imaging of cancers and other diseases. *Med. Res. Rev.* **2004**, *24*, 357–397.
- (4) Rey, A. M. Radiometal complexes in molecular imaging and therapy. *Curr. Med. Chem.* **2010**, *17*, 3673–3683.
- (5) Okarvi, S. M. Recent progress in fluorine-18 labelled peptide radiopharmaceuticals. *Eur. J. Nucl. Med.* **2001**, *28*, 929–938.
- (6) Ametamey, S. M.; Honer, M.; Schubiger, P. A. Molecular imaging with PET. *Chem. Rev.* **2008**, *108*, 1501–1516.
- (7) Vaidyanathan, G.; Zalutsky, M. R. Fluorine-18-labeled [Nle(4),D-Phe(7)]- α -MSH, an α -melanocyte stimulating hormone analogue. *Nucl. Med. Biol.* **1997**, *24*, 171–178.
- (8) Gohlke, S.; Wester, H. J.; Bruns, C.; Stocklin, G. (2-[^{18}F]Fluoropropionyl-(D)Phe(1))-Octreotide, a Potential Radiopharmaceutical for Quantitative Somatostatin Receptor Imaging with Pet—Synthesis, Radiolabeling, in Vitro Validation and Biodistribution in Mice. *Nucl. Med. Biol.* **1994**, *21*, 819–825.
- (9) Moody, T. W.; Leyton, J.; Unsworth, E.; John, C.; Lang, L. X.; Eckelman, W. C. (Arg(15),Arg(21))VIP: evaluation of biological activity and localization to breast cancer tumors. *Peptides* **1998**, *19*, 585–592.

- (10) Wester, H. J.; Hamacher, K.; Stocklin, G. A comparative study of NCA fluorine-18 labeling of proteins via acylation and photochemical conjugation. *Nucl. Med. Biol.* **1996**, *23*, 365–372.
- (11) Ting, R.; Harwig, C.; auf dem Keller, U.; McCormick, S.; Austin, P.; Overall, C. M.; Adam, M. J.; Ruth, T. J.; Perrin, D. M. Toward [(18)F]-labeled aryltrifluoroborate radiotracers: in vivo positron emission tomography imaging of stable aryltrifluoroborate clearance in mice. *J. Am. Chem. Soc.* **2008**, *130*, 12045–12055.
- (12) Honer, M.; Mu, L.; Stellfeld, T.; Graham, K.; Martic, M.; Fischer, C. R.; Lehmann, L.; Schubiger, P. A.; Ametamey, S. M.; Dinkelborg, L.; Srinivasan, A.; Borkowski, S. 18F-Labeled bombesin analog for specific and effective targeting of prostate tumors expressing gastrin-releasing peptide receptors. *J. Nucl. Med.* **2011**, *52*, 270–278.
- (13) McBride, W. J.; Sharkey, R. M.; Karacay, H.; D'Souza, C. A.; Rossi, E. A.; Laverman, P.; Chang, C. H.; Boerman, O. C.; Goldenberg, D. M. A Novel Method of F-18 Radiolabeling for PET. *J. Nucl. Med.* **2009**, *50*, 991–998.
- (14) Schirmacher, R.; Bradtmoller, G.; Schirmacher, E.; Thews, O.; Tillmanns, J.; Siessmeier, T.; Buchholz, H. G.; Bartenstein, P.; Waengler, B.; Niemeyer, C. M.; Jurkschat, K. F-18-Labeling of peptides by means of an organosilicon-based fluoride acceptor. *Angew. Chem., Int. Ed.* **2006**, *45*, 6047–6050.
- (15) Kostikov, A. P.; Chin, J.; Orchowski, K.; Niedermoser, S.; Kovacevic, M. M.; Aliaga, A.; Jurkschat, K.; Wangler, B.; Wangler, C.; Wester, H. J.; Schirmacher, R. Oxalic Acid Supported Si-F-18-Radiofluorination: One-Step Radiosynthesis of N-Succinimidyl 3-(Di-tert-butyl[F-18]fluorosilyl) benzoate ([F-18]SiFB) for Protein Labeling. *Bioconjugate Chem.* **2012**, *23*, 106–114.
- (16) Mu, L.; Hohne, A.; Schubiger, P. A.; Ametamey, S. M.; Graham, K.; Cyr, J. E.; Dinkelborg, L.; Stellfeld, T.; Srinivasan, A.; Voigtmann, U.; Klar, U. Silicon-based building blocks for one-step 18F-radiolabeling of peptides for PET imaging. *Angew. Chem., Int. Ed. Engl.* **2008**, *47*, 4922–4925.
- (17) Bohn, P.; Deyine, A.; Azzouz, R.; Bailly, L.; Fiol-Petit, C.; Bischoff, L.; Fruit, C.; Marsais, F.; Vera, P. Design of silicon-based misonidazole analogues and (18)F-radiolabelling. *Nucl. Med. Biol.* **2009**, *36*, 895–905.
- (18) Schulz, J.; Vimont, D.; Bordenave, T.; James, D.; Escudier, J. M.; Allard, M.; Szlosek-Pinaud, M.; Fouquet, E. Silicon-Based Chemistry: An Original and Efficient One-Step Approach to [F-18]-Nucleosides and [F-18]-Oligonucleotides for PET Imaging. *Chem.—Eur. J.* **2011**, *17*, 3096–3100.
- (19) Hohne, A.; Yu, L.; Mu, L.; Reiher, M.; Voigtmann, U.; Klar, U.; Graham, K.; Schubiger, P. A.; Ametamey, S. M. Organofluorosilanes as model compounds for 18F-labeled silicon-based PET tracers and their hydrolytic stability: experimental data and theoretical calculations (PET = positron emission tomography). *Chemistry* **2009**, *15*, 3736–3743.
- (20) Hohne, A.; Mu, L.; Honer, M.; Schubiger, P. A.; Ametamey, S. M.; Graham, K.; Stellfeld, T.; Borkowski, S.; Berndorff, D.; Klar, U.; Voigtmann, U.; Cyr, J. E.; Friebe, M.; Dinkelborg, L.; Srinivasan, A. Synthesis, 18F-labeling, and in vitro and in vivo studies of bombesin peptides modified with silicon-based building blocks. *Bioconjugate Chem.* **2008**, *19*, 1871–1879.
- (21) Patel, O.; Shulkes, A.; Baldwin, G. S. Gastrin-releasing peptide and cancer. *Biochim. Biophys. Acta, Rev. Cancer* **2006**, *1766*, 23–41.
- (22) Markwalder, R.; Reubi, J. C. Gastrin-releasing peptide receptors in the human prostate: relation to neoplastic transformation. *Cancer Res.* **1999**, *59*, 1152–1159.
- (23) Reile, H.; Armatis, P. E.; Schally, A. V. Characterization of High-Affinity Receptors for Bombesin/Gastrin Releasing Peptide on the Human Prostate-Cancer Cell-Lines Pc-3 and Du-145—Internalization of Receptor-Bound (125)I-(Tyr(4)) Bombesin by Tumor-Cells. *Prostate* **1994**, *25*, 29–38.
- (24) Reiher, M.; Sellmann, D.; Hess, B. A. Stabilization of diazene in Fe(II)-sulfur model complexes relevant for nitrogenase activity. I. A new approach to the evaluation of intramolecular hydrogen bond energies. *Theor. Chem. Acc.* **2001**, *106*, 379–392.
- (25) Fields, G. B.; Noble, R. L. Solid-Phase Peptide-Synthesis Utilizing 9-Fluorenylmethoxycarbonyl Amino Acids. *Int. J. Pept. Protein Res.* **1990**, *35*, 161–214.
- (26) Fiorenza, M.; Mordini, A.; Ricci, A. The Mechanism of Solvolysis of Beta-Ketosilanes. *J. Organomet. Chem.* **1985**, *280*, 177–182.
- (27) Wangler, C.; Waser, B.; Alke, A.; Iovkova, L.; Buchholz, H. G.; Niedermoser, S.; Jurkschat, K.; Fottner, C.; Bartenstein, P.; Schirmacher, R.; Reubi, J. C.; Weste, H. J.; Wangler, B. One-Step F-18-Labeling of Carbohydrate-Conjugated Octreotate Derivatives Containing a Silicon Fluoride Acceptor (SiFA): In Vitro and in Vivo Evaluation as Tumor Imaging Agents for Positron Emission Tomography (PET). *Bioconjugate Chem.* **2010**, *21*, 2289–2296.
- (28) Zhang, X. Z.; Cai, W. B.; Cao, F.; Schreiber, E.; Wu, Y.; Wu, J. C.; Xing, L.; Chen, X. Y. F-18-Labeled bombesin analogs for targeting GRP receptor-expressing prostate cancer. *J. Nucl. Med.* **2006**, *47*, 492–501.
- (29) Ahlrichs, R.; Bar, M.; Haser, M.; Horn, H.; Kolmel, C. Electronic-Structure Calculations on Workstation Computers—The Program System Turbomole. *Chem. Phys. Lett.* **1989**, *162*, 165–169.
- (30) Tao, J. M.; Perdew, J. P.; Staroverov, V. N.; Scuseria, G. E. Climbing the density functional ladder: nonempirical meta-generalized gradient approximation designed for molecules and solids. *Phys. Rev. Lett.* **2003**, *91*, 146401.
- (31) Schafer, A.; Huber, C.; Ahlrichs, R. Fully Optimized Contracted Gaussian-Basis Sets of Triple Zeta Valence Quality for Atoms Li to Kr. *J. Chem. Phys.* **1994**, *100*, 5829–5835.
- (32) Wiberg, N.; Amelunxen, K.; Lerner, H. W.; Schuster, H.; Noth, H.; Krossing, I.; Schmidt Amelunxen, M.; Seifert, T. Supersilyl alkaline metals Bu-t(3);SiM1 without or with donors—synthesis, characterization and structures. *J. Organomet. Chem.* **1997**, *542*, 1–18.
- (33) Jeganathan, A.; Richardson, S. K.; Mani, R. S.; Haley, B. E.; Watt, D. S. Selective Reactions of Azide-Substituted Alpha-Diazo Amides with Olefins and Alcohols Using Rhodium(II) Catalysts. *J. Org. Chem.* **1986**, *51*, 5362–5367.
- (34) Klingebiel, U. The 1st Lithium Fluorosilanolate—A Building Block for Directed Siloxane Synthesis. *Angew. Chem., Int. Ed. Engl.* **1981**, *20*, 678–679.
- (35) Fischer, C. R.; Muller, C.; Reber, J.; Muller, A.; Kramer, S. D.; Ametamey, S. M.; Schibli, R. [18F]Fluoro-deoxy-glucose folate: a novel PET radiotracer with improved in vivo properties for folate receptor targeting. *Bioconjugate Chem.* **2012**, *23*, 805–813.
- (36) Honer, M.; Bruhlmeier, M.; Missimer, J.; Schubiger, A. P.; Ametamey, S. M. Dynamic imaging of striatal D-2 receptors in mice using quad-HIDAC PET. *J. Nucl. Med.* **2004**, *45*, 464–470.